

Voltage-tunable integrated quantum entanglement device via nonlinear Fano resonances

Mehmet Günay¹, Priyam Das², Emre Yuce³, and Mehmet Emre Tasgin⁴

¹*Department of Nanoscience and Nanotechnology, Faculty of Arts and Science, Mehmet Akif Ersoy University, 15030 Burdur, Turkey*

²*Department of Physics, Bankura Sammilani College, Kenduadihi, Bankura, WB-722101, India*

³*Department of Physics, Middle East Technical University, 06100 Ankara, Turkey and*

⁴*Institute of Nuclear Sciences, Hacettepe University, 06800 Ankara, Turkey*

(Dated: May 26, 2022)

Integration of devices generating nonclassical states (such as entanglement) into photonic circuits is one of the major goals in achieving integrated quantum circuits (IQCs). This is demonstrated successfully in the past decades. Controlling the nonclassicality generation in these micron-scale devices is also crucial for robust operation of the IQCs. Here, we propose a micron-scale quantum entanglement device whose nonlinearity (so the generated nonclassicality) can be tuned by several orders of magnitude via an applied voltage. The level-spacing of quantum emitters (QEs), which can be tuned by voltage, are embedded into the hotspot of a metal nanostructure (MNS). QE-MNS coupling introduces a Fano resonance in the “nonlinear response”. Nonlinearity, already enhanced extremely due to localization, can be controlled by the QEs’ level-spacing. Nonlinearity can either be suppressed (also when probe is on the device) or be further enhanced by several orders. Fano resonance takes place in a relatively narrow frequency window so that \sim meV voltage-tunability for QEs becomes sufficient for a continuous turning on/off of the nonclassicality. This provides orders of magnitude modulation depths.

Quantum optics paved the way to revolutionary technologies, like quantum computation and communications, which demonstrate superior features compared to their classical counterparts. For instance, quantum computers can solve complex mathematical problems in a reasonable time which takes thousands of years in a classical supercomputer [1, 2]. Quantum networks [3], utilizing the phenomenon of quantum teleportation [4, 5], can instantly distribute data to many parties that can replace the interconnects [6] in current current processors which limit the operation frequencies [7].

Recent years witnessed the efforts on the scalable integration of the quantum optics features into photonic chips —integrated quantum circuits— which allows the operation of quantum computation and quantum communication on a single medium [8]. Such an integration (and miniaturization) necessitates the controlled generation and manipulation of entangled and/or squeezed light at much smaller (micron-scale) dimensions. This stimulated the intense research on the micron-scale generation of quantum states, for instance, quadrature-squeezed states on silicon-nitride chips [9] (continuous-variable entanglement [10–12]) and single-photon operations on semiconductor quantum dots [13–15] (discrete-variable entanglement [16]). Both approaches (also the hybrid approach [17]) utilize nonlinear interactions in a chip component. Nonlinear frequency conversion rate is either fixed [18]; or it can be controlled by auxiliary light [19], by tuning the resonances [20] and optical filters [21] (i.e., voltage-controlled preparation of two-photon states [22]), and by adjusting phase-matching condition [23]. The control on the production (switching) of quantum nonclassicality in a circuit is quite important for the robust operation of an integrated quantum circuit.

In this Letter, we study a micron-scale entangler where nonclassicality generation can not only be switched on/off, but also tuned continuously by an applied voltage. Furthermore, one can achieve modulation depths as large as several orders of magnitude. The entanglement (nonclassicality) switch is based on the Fano-control of nonlinear response of a metal nanostructure (MNS). A quantum emitter (QE) is positioned at the hot spot of the MNS and creates the Fano resonance in the nonlinear response. The level-spacing of the QE can be tuned via an applied voltage [20, 24–26], which also controls the rate of the nonlinear conversion —thus, the nonclassicality of the system. Here, as an example, we work the squeezing and entanglement generation at the fundamental frequency (ω) of a Fano-controlled second harmonic generation (SHG) process. However, such a control can be achieved also in other nonlinear processes [27, 28].

Fano resonances appear at relatively sharp frequency bands [29]. This feature may be disadvantageous in achieving broadband nonlinearity enhancements in MNSs. Here, however, we turn the sharpness of the Fano resonances into an advantage, because a smaller voltage tuning for the QE level-spacing (ω_{eg}), \sim meV [20, 24–26], comes to be sufficient for turning on and off the nonclassicality.

We consider a micron-sized photonic crystal cavity into which a MNS, e.g., a bow-tie antenna, is embedded, see Fig. 1. The QE(s), whose level-spacing is voltage-tuned [26], is positioned at the nm-sized hotspot (occurs at the gap). A Fano resonance appears due to the MNS-QE coupling, see the inset of Fig. 2. When ω_{eg} is tuned to 2ω , the SHG process (so the nonclassicality generation) is suppressed, e.g., 3-4 orders of magnitude. In contrast, when the ω_{eg} is tuned to 2.001ω , the SHG is enhanced

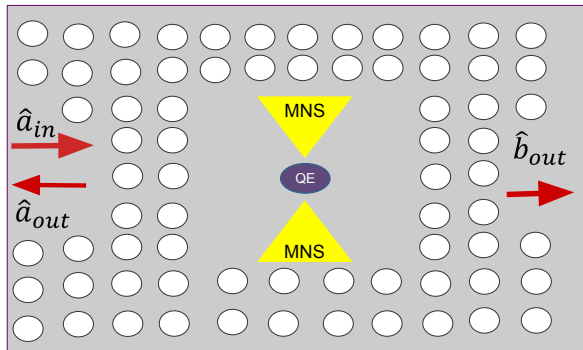


FIG. 1. Micron-scale voltage-tunable integrated entanglement device. Nonlinearity of the MNS is already extremely enhanced due to localization at the hotspot [30]. QE(s) positioned to the hotspot induces a Fano resonance which can suppress (turn off) the localization-enhanced nonlinearity by several orders at $\omega_{eg} = 2\omega$ or enhance it 10-100 times at $\omega_{eg} = 2.001$. Level-spacing (ω_{eg}) is tuned by an applied voltage [20, 24–26]. \hat{a}_{in} is the input field (integrated laser), \hat{a}_{out} and \hat{b}_{out} are the output fields whose entanglement (Fig. 2) and nonclassicality (Fig. 3) are investigated.

10-100 times. We remark that the localization (hotspot) already enhances the SHG, for instance, by 10^6 times [30]. The pronounced Fano-enhancement (suppression) factors multiplies the 10^6 localization enhancement [30, 31]. The cavity is pumped by an integrated microlaser [15, 32] on the left hand side.

Here, we show that the SHG process taking place inside the cavity (entanglement device) generates two kinds of nonclassicality. (i) The two pulses emitted from the cavity in the opposite directions (\hat{a}_{out} and \hat{b}_{out} in Fig. 1), at the fundamental frequency ω , are entangled, see Fig. 2. (ii) The transmitted light \hat{b}_{out} is single-mode nonclassical, see Fig. 3. Thus, one can either (i) use the two entangled light beams or (ii) create entanglement (on the right hand side) from the nonclassicality inherited in \hat{b}_{out} using an integrated beam-splitter[33]. Beyond the generation of nonclassicality [34, 35], the most important thing our device can provide is the continuous tunability of the quantum nonclassicality (by several orders of magnitude) via an applied voltage.

Cavity system and hamiltonian.— Dynamics of the voltage-controlled entanglement device can be described as follows. An integrated laser of frequency ω excites the fundamental cavity mode (\hat{c}_1) on the left hand side, $\hat{\mathcal{H}}_L = \hbar\varepsilon_L(\hat{c}_1^\dagger e^{-i\omega t} + H.c.)$. The cavity mode couples with the first (lower-energy) plasmon mode (\hat{a}_1 , resonance Ω_1) of the bow-tie MNS, $\hat{\mathcal{H}}_1 = \hbar g_1 \hat{a}_1^\dagger \hat{c}_1 + H.c.$. The \hat{a}_1 plasmon excitation is localized within the nm-sized hotspot located at the gap between the two metal nanoparticles. Orders of magnitude enhanced electromagnetic field (ω), at the hotspot, yield the SHG process [36]. Two local-

ized excitations (ω) in the \hat{a}_1 plasmon mode combine to produce a single 2ω plasmon in the second (higher energy) plasmon mode \hat{a}_2 , $\hat{\mathcal{H}}_{SHG} = \hbar\chi^{(2)}\hat{a}_2^\dagger\hat{a}_1\hat{a}_1 + H.c.$. The hotspot of the \hat{a}_2 mode, of resonance Ω_2 , is also at the center (gap). The SHG conversion takes place over the plasmons [37] because overlap integral for this process is extremely larger due to the localization [31, 38]. As both incident (ω) and converted (2ω) fields are localized the SHG process can be enhanced as large as 10^6 times — localization enhancement [30]. The level-spacing of the QE (ω_{eg}) is around the second harmonic (SH) frequency 2ω and the resonance Ω_2 of the second plasmon mode \hat{a}_2 , so that it is off-resonant to the fundamental frequency. The localized \hat{a}_2 plasmon mode couples with the QE(s) ($\hat{\mathcal{H}}_2 = \hbar f|e\rangle\langle g|\hat{a}_2 + H.c.$), which introduces a Fano resonance in the SH conversion, see inset of Fig. 2. The SHG process can be controlled by the level-spacing of the QE(s), ω_{eg} which is tuned by an applied voltage [26]. When voltage tunes to $\omega_{eg} = 2\omega$, the localization enhanced (e.g., about 10^6 times) SHG is suppressed, for instance, 10^{-4} times. That is, the switch turns the SHG off. When $\omega_{eg} \simeq 2.001\omega$, this time the localization enhanced SHG is further multiplied by a factor of $\sim 10\text{-}10^2$.

The SHG process ($\hat{a}_2^\dagger\hat{a}_1\hat{a}_1 + H.c.$) generates the nonclassicality (e.g., squeezing) in the \hat{a}_1 plasmon mode. The nonclassicality of the \hat{a}_1 mode is transferred back to the fundamental cavity mode \hat{c}_1 via the beam splitter like interaction. Nonclassicality introduces in the \hat{c}_1 mode. The cavity mode couples to the left (\hat{a}_{out}) and right (\hat{b}_{out}) hand sides of the cavity. \hat{a}_{out} and \hat{b}_{out} are related to the cavity field \hat{c}_1 via input-output relations [39]. Because of the common interaction with the cavity mode (entanglement swap [40]) and the nonclassicality of \hat{c}_1 , the \hat{a}_{out} and \hat{b}_{out} modes get entangled, see Fig. 2. In addition to this entanglement, the nonclassicality (squeezing) in the cavity mode is transferred also to the \hat{b}_{out} on the right hand side. Thus, \hat{b}_{out} is also single-mode nonclassical (squeezed) as well as it is entangled with the \hat{a}_{out} mode. (Not all of the total nonclassicality can be converted into entanglement in beam-splitter like interactions, but some single-mode nonclassicality remains within the transferred mode [41].) One does not have to use the entanglement of the \hat{a}_{out} and \hat{b}_{out} modes, but can also convert the single-mode nonclassicality of the transmitted \hat{b}_{out} mode into entanglement by placing an integrated beam splitter on the right hand side [42].

Langevin equations.— Time evolution of the operators can be determined using the Heisenberg equations of motion, e.g., $\dot{\hat{a}}_1 = [\hat{a}_1, \hat{\mathcal{H}}]$ as

$$\dot{\hat{c}}_1 = -(\kappa_1 + i\omega_1)\hat{c}_1 - ig_1^*\hat{a}_1 + \varepsilon_{LE}e^{-i\omega t}, \quad (1)$$

$$\dot{\hat{c}}_2 = -(\kappa_2 + i\omega_2)\hat{c}_2 - ig_2^*\hat{a}_2, \quad (2)$$

$$\dot{\hat{a}}_1 = -(\gamma_1 + i\Omega_1)\hat{a}_1 - ig_1\hat{c}_1 - i2\chi^{(2)}\hat{a}_1^\dagger\hat{a}_2, \quad (3)$$

$$\dot{\hat{a}}_2 = -(\gamma_2 + i\Omega_2)\hat{a}_2 - ig_2\hat{c}_2 - i\chi^{(2)}\hat{a}_1^2 - if\hat{\rho}_{ge}, \quad (4)$$

$$\dot{\hat{\rho}}_{ge} = -(\gamma_{eg} + i\omega_{eg})\hat{\rho}_{ge} + if\hat{a}_2(\hat{\rho}_{ee} - \hat{\rho}_{gg}), \quad (5)$$

$$\dot{\hat{\rho}}_{ee} = -\gamma_{ee}\hat{\rho}_{ee} + i2f(\hat{a}_2^\dagger\hat{\rho}_{eg} - H.c.), \quad (6)$$

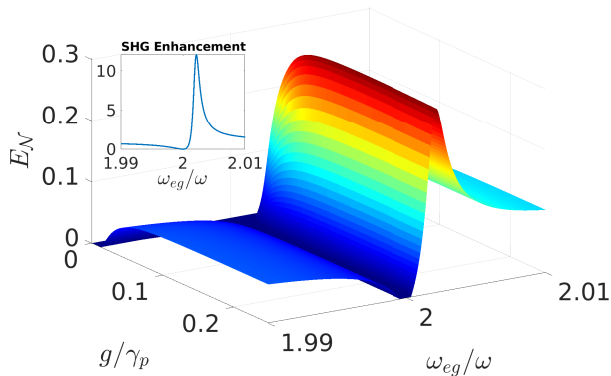


FIG. 2. Degree of the entanglement (log-neg) of the two output fields δa_{out} and δb_{out} in Fig. 1. Voltage-tuning of the QE(s) level-spacing between $\omega_{eg} = 2\omega$ and $\omega_{eg} = 2.001\omega$ turns on and off the entanglement, thus an undesired pulse is not turned into nonclassical. (Inset.) Fano-enhancement of the SHG, which multiplies the localization enhancement [30], for different ω_{eg} .

where $\kappa_{1,2}$ and $\gamma_{1,2}$ are the decay rates for the cavity and plasmon modes. γ_{ee} , and γ_{eg} are the diagonal and off-diagonal decay rates of the QE(s). Please see Supp. Mat. [43] for details.

Fano control.— One can find the field amplitudes of the coupled cavity-MNS-QE(s) system examining the expectations of the operators, e.g., $\alpha_{1,2} = \langle \hat{a}_{1,2} \rangle$. Here, $|\alpha_2|^2$ gives the number of SH converted plasmons which governs the nonclassicality of the system. The steady-state amplitude of the second harmonic plasmons [44]

$$\alpha_2 = \frac{i\chi^{(2)}}{\frac{|f|^2 y}{i(\omega_{eg}-2\omega)+\gamma_{eg}} - [i(\Omega_2 - 2\omega) + \gamma_2]} \alpha_1^2 \quad (7)$$

is governed by the interference taking place in the denominator $\mathcal{D}(\omega) = \frac{|f|^2 y}{i(\omega_{eg}-2\omega)+\gamma_{eg}} - [i(\Omega_2 - 2\omega) + \gamma_2]$. When $\omega_{eg} = 2\omega$, the first term of \mathcal{D} becomes $|f|^2 y / \gamma_{eg}$ which turns out to be very large due to the QE's small decay rate [20], e.g., $\gamma_{eg} = 10^{-6}\omega$. The typical values for MNS-QE coupling and population inversion are $f = 0.05\omega$ and $y = \rho_{ee} - \rho_{gg} \sim -1$. Thus, the first term of \mathcal{D} becomes of order $\sim 10^4\omega$ while the second term of \mathcal{D} is less than unity ($1 \times \omega$). This greatly suppresses the SHG which is depicted in the inset of Fig. 2. We remark that without the presence of the QE, the SHG of the MNS is governed by the second term of \mathcal{D} . The suppression is stronger when sharper resonance QE(s) are used.

In contrast, one can also enhance the SHG by performing a cancellation in the denominator \mathcal{D} . By tuning ω_{eg} accordingly, the off-resonant expression $(\Omega_2 - 2\omega)$ can be canceled by the imaginary part of the first term in \mathcal{D} , see $\omega_{eg} = 2.001\omega$ in the inset of Fig. 2. Therefore, tuning the level-spacing of the QE ω_{eg} about $\sim \text{meV}$ one can continuously tune the SHG by 5-orders of magnitude and in particular turn on and off the nonclassicality. We

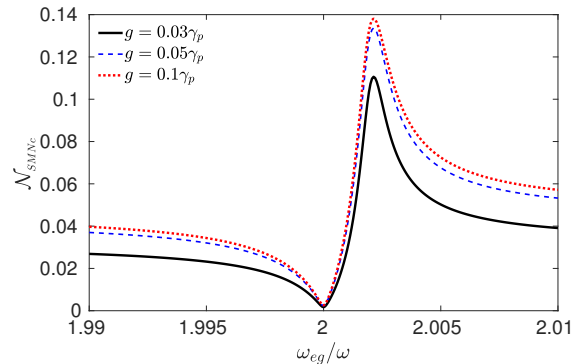


FIG. 3. Single-mode nonclassicality ($\mathcal{N}_{\text{SMNC}}$) of the output mode \hat{b}_{out} in units of log-neg [34, 45]. The right-going output can be used to generate entanglement via a beam-splitter [42]. Nonclassicality is depicted for different cavity-MNS coupling strengths $g = 0.03\gamma_p$ (black-solid line), $g = 0.05\gamma_p$ (blue-dashed line) and $g = 0.1\gamma_p$ (red-dotted line).

utilize this phenomenon as voltage-controlled integrable quantum entanglement device.

Nonclassicality and Entanglement.— We calculate the nonclassicality of the system using the standard (quantum noise) methods [39]. The quantum nonclassicality features of a system is determined solely by the fluctuations [46] (noise, e.g., $\delta \hat{a}_1$) around the expectations values of the fields ($\alpha_1 = \langle \hat{a}_1 \rangle$), i.e., $\hat{a}_1 = \alpha_1 + \delta \hat{a}_1$ and $\hat{c}_1 = \beta_1 + \delta \hat{c}_1$. The Langevin equations for the noise operators can be written as

$$\delta \dot{\hat{c}}_1 = -[\kappa_1 + i(\omega_1 - \omega)]\delta \hat{c}_1 - ig_1^* \delta \hat{a}_1 + \delta \hat{c}_{in}^{(1)}, \quad (8a)$$

$$\delta \dot{\hat{c}}_2 = -[\kappa_2 + i(\omega_2 - 2\omega)]\delta \hat{c}_2 - ig_2^* \delta \hat{a}_2 + \delta \hat{c}_{in}^{(2)}, \quad (8b)$$

$$\delta \dot{\hat{a}}_1 = -[\Gamma_1 + i(\Omega_1 - \omega)]\delta \hat{a}_1 - ig_1 \delta \hat{c}_1 - 2i\chi^{(2)}(\alpha_1^* \delta \hat{a}_2 + \alpha_2 \delta \hat{a}_1), \quad (8c)$$

$$\delta \dot{\hat{a}}_2 = -[\Gamma_2 + i(\Omega_2 - 2\omega)]\delta \hat{a}_2 - ig_2 \delta \hat{c}_2 - i\chi^{(2)}(2\alpha_1 \delta \hat{a}_1). \quad (8d)$$

Quantum optics experiments with MNSs [47–51] demonstrate that, intriguingly, plasmon excitations can hold entanglement much longer times [47–50, 52, 53] compared to their decay rates controlling field amplitudes. For this reason, empirically, we need to consider a smaller decoherence rate $\Gamma_{1,2}$ for the noise operators $\delta \hat{a}_{1,2}$. (We also present our results with $\Gamma_{1,2} = \gamma_{1,2}$ in the SM [43] for convenience, though not reliable physically.)

First, we calculate the entanglement between the reflected (\hat{a}_{out}) and transmitted (\hat{b}_{out}) pulses, see Fig. 1. We calculate the logarithmic-negativity ($E_{\mathcal{N}}$), which is an entanglement measure for Gaussian states [54]. As we use the standard linearization method [39] for calculating the evolution of the noise operators, the fields stay Gaussian and $E_{\mathcal{N}}$ can be employed as a measure. In Fig. 2, we observe that the log-neg can be tuned continuously on and off between $\omega_{eg} = 2\omega$ and $\omega_{eg} = 2.001\omega$.

Next, we also calculate the single-mode nonclassicality of the transmitted wave \hat{b}_{out} . We employ the entanglement potential [55] as measure for the single-mode nonclassicality. Only a nonclassical single-mode state can create entanglement at the output of a beam-splitter [42]. Entanglement potential is the degree of entanglement a nonclassical state creates at the beam-splitter output which can also be quantified in terms of log-neg. We remind that not all of the nonclassicality of a mode could be converted into entanglement at the beam splitter output. In Fig. 3, we observe that $\mathcal{N}_{\text{SMNC}}$ can similarly be continuously tuned by several orders of magnitude via a \sim meV adjustment of the QE level-spacing. Such a modulation in the quantized energy level spacing of the colloidal quantum dots up to 25 meV is succeeded in Ref. [24].

Therefore, one can use the (i) entanglement of two pulses propagating in opposite directions or (ii) convert the nonclassicality of the transmitted \hat{b}_{out} pulse into entanglement on the right hand side using an integrated beam splitter. Such a modulation is important for gen-

erating the nonclassicality when the desired pulse is passing through the device, but turning it off for an unwanted pulse. We note that the sample setup, Fig. 1, can also be placed into a smaller cavity [56].

In summary, we introduce a micron-scale quantum entanglement device which can be integrated into (quantum) photonic circuits. The nonclassicality can be supplied into the integrated quantum circuit on demand by applying a voltage on the device. Unlike the integrable quadrature squeezing generators presented in the literature [9, 57–59], the nonclassicality can be turned off also when a pulse is passing through the device. The voltage can also continuously tune the degree of the generated entanglement/nonclassicality. The linear response of the device is not altered by voltage. Although we study the tuning of nonclassicality on a second harmonic generation process here, the same method can be applied also on the the voltage-tuning of other nonlinear processes. The details of our calculations following the standard methods can be found in the SM [43].

-
- [1] H.-S. Zhong, H. Wang, Y.-H. Deng, M.-C. Chen, L.-C. Peng, Y.-H. Luo, J. Qin, D. Wu, X. Ding, Y. Hu, *et al.*, Quantum computational advantage using photons, *Science* **370**, 1460 (2020).
- [2] A. W. Harrow and A. Montanaro, Quantum computational supremacy, *Nature* **549**, 203 (2017).
- [3] H. J. Kimble, The quantum internet, *Nature* **453**, 1023 (2008).
- [4] C. H. Bennett, G. Brassard, C. Crépeau, R. Jozsa, A. Peres, and W. K. Wootters, Teleporting an unknown quantum state via dual classical and Einstein-Podolsky-Rosen channels, *Physical review letters* **70**, 1895 (1993).
- [5] X.-H. Jiang, P. Chen, K.-Y. Qian, Z.-Z. Chen, S.-Q. Xu, Y.-B. Xie, S.-N. Zhu, and X.-S. Ma, Quantum teleportation mediated by surface plasmon polariton, *Scientific Reports* **10**, 1 (2020).
- [6] D. Awschalom, K. K. Berggren, H. Bernien, S. Bhavne, L. D. Carr, P. Davids, S. E. Economou, D. Englund, A. Faraon, M. Fejer, *et al.*, Development of quantum interconnects (quics) for next-generation information technologies, *PRX Quantum* **2**, 017002 (2021).
- [7] E. Ozbay, Plasmonics: merging photonics and electronics at nanoscale dimensions, *Science* **311**, 189 (2006).
- [8] A. W. Elshaari, W. Pernice, K. Srinivasan, O. Benson, and V. Zwiller, Hybrid integrated quantum photonic circuits, *Nature Photonics* **14**, 285 (2020).
- [9] V. D. Vaidya, B. Morrison, L. Helt, R. Shahrokshahi, D. Mahler, M. Collins, K. Tan, J. Lavoie, A. Repington, M. Menotti, *et al.*, Broadband quadrature-squeezed vacuum and nonclassical photon number correlations from a nanophotonic device, *Science Advances* **6**, eaba9186 (2020).
- [10] S. L. Braunstein and P. Van Loock, Quantum information with continuous variables, *Reviews of Modern Physics* **77**, 513 (2005).
- [11] W. P. Bowen, R. Schnabel, P. K. Lam, and T. C. Ralph, Experimental investigation of criteria for continuous variable entanglement, *Physical Review Letters* **90**, 043601 (2003).
- [12] G. Masada, K. Miyata, A. Politi, T. Hashimoto, J. L. O’Brien, and A. Furusawa, Continuous-variable entanglement on a chip, *Nature Photonics* **9**, 316 (2015).
- [13] H. Wang, Y. He, Y.-H. Li, Z.-E. Su, B. Li, H.-L. Huang, X. Ding, M.-C. Chen, C. Liu, J. Qin, *et al.*, High-efficiency multiphoton boson sampling, *Nature Photonics* **11**, 361 (2017).
- [14] J. C. Lored, M. A. Broome, P. Hilaire, O. Gazzano, I. Sagnes, A. Lemaitre, M. P. Almeida, P. Senellart, and A. G. White, Boson sampling with single-photon fock states from a bright solid-state source, *Phys. Rev. Lett.* **118**, 130503 (2017).
- [15] S. Rodt and S. Reitzenstein, Integrated nanophotonics for the development of fully functional quantum circuits based on on-demand single-photon emitters, *APL Photonics* **6**, 010901 (2021).
- [16] S. Takeda, M. Fuwa, P. van Loock, and A. Furusawa, Entanglement swapping between discrete and continuous variables, *Physical Review Letters* **114**, 100501 (2015).
- [17] U. L. Andersen, J. S. Neergaard-Nielsen, P. Van Loock, and A. Furusawa, Hybrid discrete-and continuous-variable quantum information, *Nature Physics* **11**, 713 (2015).
- [18] Y. Zhao, Y. Okawachi, J. K. Jang, X. Ji, M. Lipson, and A. L. Gaeta, Near-degenerate quadrature-squeezed vacuum generation on a silicon-nitride chip, *Physical Review Letters* **124**, 193601 (2020).
- [19] X. Lu, G. Moille, A. Rao, D. A. Westly, and K. Srinivasan, Efficient photoinduced second-harmonic generation in silicon nitride photonics, *Nature Photonics* **15**, 131 (2021).
- [20] D. Hallett, A. P. Foster, D. L. Hurst, B. Royall, P. Kok, E. Clarke, I. E. Itskevich, A. M. Fox, M. S. Skolnick, and L. R. Wilson, Electrical control of nonlinear quantum optics in a nano-photon waveguide, *Optica* **5**, 644

- (2018).
- [21] A. Foster, D. Hallett, I. Iorsh, S. Sheldon, M. Godland, B. Royall, E. Clarke, I. Shelykh, A. Fox, M. Skolnick, *et al.*, Tunable photon statistics exploiting the fano effect in a waveguide, *Physical Review Letters* **122**, 173603 (2019).
- [22] T. Heindel, A. Thoma, M. von Helversen, M. Schmidt, A. Schlehahn, M. Gschrey, P. Schnauber, J.-H. Schulze, A. Strittmatter, J. Beyer, *et al.*, A bright triggered twin-photon source in the solid state, *Nature Communications* **8**, 1 (2017).
- [23] M. Wang, N. Yao, R. Wu, Z. Fang, S. Lv, J. Zhang, J. Lin, W. Fang, and Y. Cheng, Strong nonlinear optics in on-chip coupled lithium niobate microdisk photonic molecules, *New Journal of Physics* **22**, 073030 (2020).
- [24] K. Shibata, H. Yuan, Y. Iwasa, and K. Hirakawa, Large modulation of zero-dimensional electronic states in quantum dots by electric-double-layer gating, *Nature Communications* **4**, 1 (2013).
- [25] C. Chakraborty, L. Kinnischtzke, K. M. Goodfellow, R. Beams, and A. N. Vamivakas, Voltage-controlled quantum light from an atomically thin semiconductor, *Nature Nanotechnology* **10**, 507 (2015).
- [26] S. Schwarz, A. Kozikov, F. Withers, J. Maguire, A. Foster, S. Dufferwiel, L. Hague, M. Makhonin, L. Wilson, A. Geim, *et al.*, Electrically pumped single-defect light emitters in WSe₂, *2D Materials* **3**, 025038 (2016).
- [27] S. K. Singh, M. K. Abak, and M. E. Tasgin, Enhancement of four-wave mixing via interference of multiple plasmonic conversion paths, *Phys. Rev. B* **93**, 035410 (2016).
- [28] M. Günay, A. Cicek, N. Korozlu, A. Bek, and M. E. Tasgin, Fano enhancement of unlocalized nonlinear optical processes, *Phys. Rev. B* **104**, 235407 (2021).
- [29] S. Postaci, B. C. Yildiz, A. Bek, and M. E. Tasgin, Silent enhancement of SERS signal without increasing hot spot intensities, *Nanophotonics* **7**, 1687 (2018).
- [30] M. Celebrano, X. Wu, M. Baselli, S. Großmann, P. Bigioni, A. Locatelli, C. De Angelis, G. Cerullo, R. Osellame, B. Hecht, *et al.*, Mode matching in multiresonant plasmonic nanoantennas for enhanced second harmonic generation, *Nature Nanotechnology* **10**, 412 (2015).
- [31] E. Kamenetskii, A. Sadreev, and A. Miroshnichenko, Fano resonances in optics and microwaves, *Springer Series in Optical Sciences Book Series* (2018).
- [32] P. Munnely, T. Heindel, A. Thoma, M. Kamp, S. Höfling, C. Schneider, and S. Reitzenstein, Electrically tunable single-photon source triggered by a monolithically integrated quantum dot microlaser, *ACS Photonics* **4**, 790 (2017).
- [33] M. Hillery and M. S. Zubairy, Entanglement conditions for two-mode states: Applications, *Phys. Rev. A* **74**, 032333 (2006).
- [34] M. E. Tasgin, Measuring nonclassicality of single-mode systems, *Journal of Physics B: Atomic, Molecular and Optical Physics* **53**, 175501 (2020).
- [35] M. E. Tasgin, M. Gunay, and M. S. Zubairy, Nonclassicality and entanglement for wave packets, *Phys. Rev. A* **101**, 062316 (2020).
- [36] C. Hubert, L. Billot, P.-M. Adam, R. Bachelot, P. Royer, J. Grand, D. Gindre, K. Dorkenoo, and A. Fort, Role of surface plasmon in second harmonic generation from gold nanorods, *Applied Physics Letters* **90**, 181105 (2007).
- [37] N. B. Grosse, J. Heckmann, and U. Woggon, Nonlinear plasmon-photon interaction resolved by *k*-space spectroscopy, *Phys. Rev. Lett.* **108**, 136802 (2012).
- [38] M. Kauranen and A. V. Zayats, Nonlinear plasmonics, *Nature Photonics* **6**, 737 (2012).
- [39] C. Genes, A. Mari, P. Tombesi, and D. Vitali, Robust entanglement of a micromechanical resonator with output optical fields, *Physical Review A* **78**, 032316 (2008).
- [40] A. Sen, U. Sen, Č. Brukner, V. Bužek, M. Żukowski, *et al.*, Entanglement swapping of noisy states: A kind of superadditivity in nonclassicality, *Phys. Rev. A* **72**, 042310 (2005).
- [41] W. Ge, M. E. Tasgin, and M. S. Zubairy, Conservation relation of nonclassicality and entanglement for gaussian states in a beam splitter, *Phys. Rev. A* **92**, 052328 (2015).
- [42] M. S. Kim, W. Son, V. Bužek, and P. L. Knight, Entanglement by a beam splitter: Nonclassicality as a prerequisite for entanglement, *Phys. Rev. A* **65**, 032323 (2002).
- [43] See Supplemental Material.
- [44] M. Günay, Z. Artvin, A. Bek, and M. E. Tasgin, Controlling steady-state second harmonic signal via linear and nonlinear Fano resonances, *Journal of Modern Optics* **67**, 26 (2020).
- [45] J. K. Asbóth, J. Calsamiglia, and H. Ritsch, Computable measure of nonclassicality for light, *Physical Review Letters* **94**, 173602 (2005).
- [46] R. Simon, N. Mukunda, and B. Dutta, Quantum-noise matrix for multimode systems: U(n) invariance, squeezing, and normal forms, *Phys. Rev. A* **49**, 1567 (1994).
- [47] S. Fasel, M. Halder, N. Gisin, and H. Zbinden, Quantum superposition and entanglement of mesoscopic plasmons, *New Journal of Physics* **8**, 13 (2006).
- [48] A. Huck, S. Smolka, P. Lodahl, A. S. Sørensen, A. Boltasseva, J. Janousek, and U. L. Andersen, Demonstration of quadrature-squeezed surface plasmons in a gold waveguide, *Physical Review Letters* **102**, 246802 (2009).
- [49] S. Varró, N. Kroó, D. Oszetzky, A. Nagy, and A. Czitzovszky, Hanbury brown–twiss type correlations with surface plasmon light, *Journal of Modern Optics* **58**, 2049 (2011).
- [50] G. Di Martino, Y. Sonnefraud, S. Kéna-Cohen, M. Tame, S. K. Özdemir, M. Kim, and S. A. Maier, Quantum statistics of surface plasmon polaritons in metallic stripe waveguides, *Nano Letters* **12**, 2504 (2012).
- [51] J. R. Krenn, A. Dereux, J.-C. Weeber, E. Bourillot, Y. Lacroute, J.-P. Goudonnet, G. Schider, W. Gotschy, A. Leitner, F. R. Aussenegg, *et al.*, Squeezing the optical near-field zone by plasmon coupling of metallic nanoparticles, *Physical Review Letters* **82**, 2590 (1999).
- [52] S. Fasel, F. Robin, E. Moreno, D. Erni, N. Gisin, and H. Zbinden, Energy-time entanglement preservation in plasmon-assisted light transmission, *Phys. Rev. Lett.* **94**, 110501 (2005).
- [53] M. S. Tame, K. McEnery, Ş. Özdemir, J. Lee, S. A. Maier, and M. Kim, Quantum plasmonics, *Nature Physics* **9**, 329 (2013).
- [54] M. B. Plenio, Logarithmic negativity: A full entanglement monotone that is not convex, *Phys. Rev. Lett.* **95**, 090503 (2005).
- [55] J. K. Asbóth, J. Calsamiglia, and H. Ritsch, Computable measure of nonclassicality for light, *Phys. Rev. Lett.* **94**, 173602 (2005).
- [56] Y. Akahane, T. Asano, B.-S. Song, and S. Noda, High-q photonic nanocavity in a two-dimensional photonic crystal, *nature* **425**, 944 (2003).

- [57] F. Mondain, T. Lunghi, A. Zavatta, E. Gouzien, F. Doutre, M. D. Micheli, S. Tanzilli, and V. D'Auria, Chip-based squeezing at a telecom wavelength, *Photon. Res.* **7**, A36 (2019).
- [58] Y. Zhang, M. Menotti, K. Tan, V. Vaidya, D. Mahler, L. Helt, L. Zatti, M. Liscidini, B. Morrison, and Z. Ver-
non, Squeezed light from a nanophotonic molecule, *Nature Communications* **12**, 1 (2021).
- [59] F. Lenzini, J. Janousek, O. Thearle, M. Villa, B. Haylock, S. Kasture, L. Cui, H.-P. Phan, D. V. Dao, H. Yonezawa, *et al.*, Integrated photonic platform for quantum information with continuous variables, *Science Advances* **4**, eaat9331 (2018).